Fracture Mechanics of Concrete Structures, de Borst et al (eds) © 2001 Swets & Zeitlinger, Lisse, ISBN 90 2651 825 0

Effect of Type and Volume Fraction of Aggregate on the Fracture Properties of Concrete

M.A.Tasdemir
Faculty of Civil Engineering, Istanbul Technical University, Istanbul, Turkey
B.L.Karihaloo
Division of Civil Engineering, Cardiff University, Cardiff, UK

ABSTRACT: Fine and coarse aggregates play a vital role in the fracture of concrete. There is however little quantitative information available in the literature on the effect of the volume fraction of the aggregates on the fracture properties of concrete. The main objective of this work is to gain a better understanding of this effect using appropriate experiment and a meso-mechanical approach. For this, several control mixes ranging from hardened cement paste (hcp) to normal concrete were prepared in which the aggregate grading, water to cement ratio, and the maximum particle size of aggregate were kept constant, but the volume fraction of aggregate was varied from 0.0 (hcp) to 0.60 in steps of 0.15.

The critical stress intensity factor of the hardened cement paste, for which LEFM is valid, was determined from centrally notched disc specimens. The effective stress intensity factors of fine mortar, coarse mortar and concrete were then calculated from that of hcp using the appropriate toughening mechanism in meso-mechanical relations. The specific fracture energies, the macro-tensile strengths and the moduli of elasticity of fine mortar, coarse mortar, and concrete were also calculated from meso-mechanical relationships.

It is shown that the meso-mechanical modelling approach gives a clear qualitative and quantitative picture of how a brittle matrix (i.e. hcp) progressively transforms into a tougher, stiffer and more ductile composite as the volume fraction of fine and coarse aggregates is increased without altering their grading.

1 INTRODUCTION

As concrete is a widely used material in structural engineering, engineers need information on the factors that influence crack initiation and propagation in the material. This information is especially needed for the numerical analysis of concrete behaviour. There is a growing interest in the field of fracture mechanics of concrete. Although intensive studies on fracture of this material have been conducted during the past three decades, some fundamental aspects of the fracture process in concrete still remain unclear because of the heterogeneity of the material. Recent advances show that a single fracture parameter, such as the critical stress intensity factor cannot adequately describe the fracture of quasi-brittle materials like concrete. This inapplicability of the conventional linear elastic fracture mechanics (LEFM) is due to the toughening mechanisms present in concrete.

Since aggregate occupies about 75 percent of the total volume of concrete it is not surprising that this constituent plays an important role in the fracture of the material. Most investigations, however, have mainly concentrated on the effect of the aggregate particle shape and size, surface texture, and water absorption. In recent years, the effect of both the aggregate type and its size on the mechanical properties of concrete were investigated by several researchers (Aitcin & Mehta, 1990; Baalbaki et al., 1991; Tasdemir et al., 1999; Sengül, et al., 2000). It is well established that the amount of crack bridging is determined by the maximum size of aggregates and that a longer tail is an indication of enhanced cracking both in size and number (van Mier, 1991; Tasdemir et al., 1995). The effect of the maximum size of aggregate on both the fracture energy and the brittleness may be important, if the crack surface roughness induces aggregate interlock, and as a result, concrete absorbs more energy (Karihaloo, 1995). It was recently indicated that as the maximum size of aggregate increases, the characteristic length increases significantly, i.e. concrete exhibits significantly more ductile behaviour. Little information, however, is available on the effect of aggregate volume fraction on the fracture properties of concrete.

The main objective of this work is to determine the effect of aggregate volume fraction on the fracture and mechanical properties of concrete. For this purpose, a meso-mechanical model based on fracture mechanics is used for gaining a better understanding of the material behaviour. This modelling technique will also improve substantially

our knowledge of how a brittle material such as hardened cement paste transforms to a quasi-brittle (i.e. ductile) concrete.

2 TRANSITION FROM BRITTLE TO QUASI-BRITTLE

Concrete is a very complex heterogeneous system. For the meso-mechanical modelling purposes, it can be regarded as a three-phase composite material consisting of the aggregate, the hardened cement paste and the interface between these two phases (Neville, 1997). It is well known that both the aggregate and the hardened cement paste show almost linear elastic brittle behaviour when they are separately subjected to a typical uniaxial compressive loading, as shown in Figure 1. The stress-strain relation of normal concrete, however, has a typical curvature under the same loading conditions. The reason for this curvature is the presence of interfaces between the aggregate and cement paste from which the first cracks form upon loading. As the load is further increased these bond cracks penetrate into the matrix. Thus an interconnected network of bond and matrix cracks form in the material until eventual failure (Tasdemir et al., 1996).

For the modelling purposes, Wittmann (1983) introduced the idea of three levels of observation: micro-, meso- and macro levels. For establishing a realistic fracture model at the macro-level in concrete, an insight into the fracture mechanisms at the meso-level is required, because it is at this level that heterogeneity results in a non-uniform internal strain distribution within the concrete composite. Recent research (Skalny, 1989; Larbi, 1993; Sarkar, 1994) has shown that there are two principal approaches to studying the interfaces in concrete: i) the micro-structural approach of including the interfacial region and its effect on concrete properties; and ii) continuum and fracture mechanics approaches to studying the effect of interfaces on the properties of concrete. In the present work, concrete is considered from the fracture mechanics point of view.

To obtain quantitative results, some transition concrete mixes were evaluated in the light of the material model used. In all mixes, the grading of concrete, water-cement ratio, and maximum particle size of aggregate were kept constant, but the volume fraction was varied from 0.15 to 0.60. Details of the transition materials and experiments are given below.

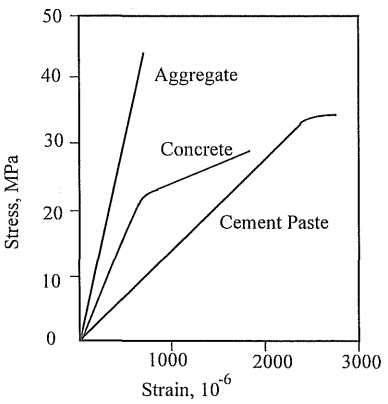

Figure 1. Typical stress-strain relations for cement paste, aggregate and concrete (After Neville, 1997)

3 TOUGHENING MECHANISMS

Linear elastic fracture mechanics predicts that the stress goes to infinity at a crack tip, which is not possible in a real material such as concrete. There is an inelastic zone in front of the visible crack. To quantify this behaviour, the Fictitious Crack Model for the fracture behaviour of concrete was proposed by Hillerborg et al. (1976). This model is extensively used in finite element analysis and other fracture mechanics based modelling. It replaces the so-called process zone ahead of a visible crack by a "fictitious" crack.

Some toughening mechanisms representing energy dissipation processes in concrete are shown in Figure 2. These are crack shielding, crack

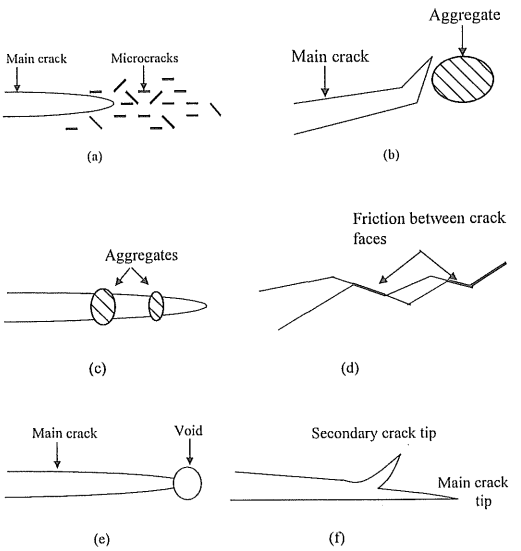

Figure 2. Some toughening mechanisms in fracture process zone: (a) crack shielding, (b) crack deflection, (c) aggregate bridging, (d) crack surface roughness-induced closure, (e) crack tip blunted by void, and (f) crack branching (After Shah et al., 1995)

deflection, aggregate bridging, crack surface roughness induced closure, crack tip blunting by voids and crack branching mechanisms (Shah et al., 1995). One of the main toughening mechanisms is aggregate bridging; it occurs when the crack has advanced beyond an aggregate to transmit the stress across the crack resulting in grain pullout. This mechanism causes energy dissipation through friction. In the meso-mechanical relations, these mechanisms of toughening are included. Application of the meso-mechanical model used for concretes will be explained below.

4 MESO-MECHANICAL RELATIONS

To evaluate the fracture parameters of cementitious materials ranging from brittle hardened cement paste to real concrete, the meso-mechanical relations developed by Karihaloo (1995), Lange-Kornbak and Karihaloo (1996, 1999), Karihaloo et al. (1991), and Huang and Li (1989) were used. The latter authors constructed the tension-softening curve from two separate curves as illustrated in Figure 3, the second part resulting from the frictional pull-out of the aggregates, $0 \le \sigma \le \sigma_f$.

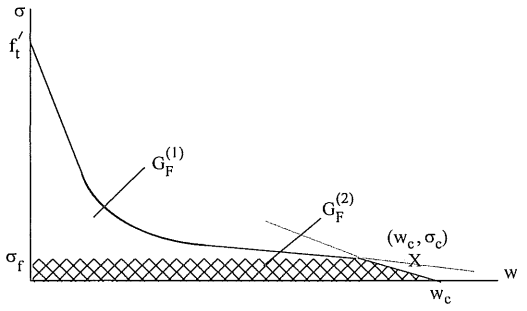

Figure 3. A typical tension-softening curve of concrete (After Huang & Li, 1989)

Thus fracture energy G_F can be written as

$$G_F = G_F^{(1)} + G_F^{(2)} + \int_{\sigma=0_f}^{f_t} w(\sigma)d\sigma + \int_{\sigma=0}^{\sigma_f} w(\sigma)d\sigma \qquad (1)$$

where

$$G_F^{(1)} = \frac{(K_{Ic})^2(1-\nu^2)}{E(1-V_{agg})}\left\{\frac{1}{3}\left[\left(\frac{K_f}{\sqrt{\frac{2}{\pi}}K_{Ic}}\right)^3 - 1\right] - \ln\left(\frac{K_f}{\sqrt{\frac{2}{\pi}}K_{Ic}}\right)\right\} \qquad (2)$$

and

$$G_F^{(2)} = \int_{\sigma=0}^{\sigma_f}\left(\sqrt{\eta g} - \frac{g}{3\tau^* V_{agg}}\sigma\right)d\sigma = \sqrt{\eta}K_f - K_f^2/(6\tau^* V_{agg})$$

In the above equations, ν is Poisson's ratio, E is effective modulus of elasticity, K_{Ic} is effective fracture toughness, η is surface texture parameter of the aggregate with the dimension of length, τ^* is shear strength of the aggregate-matrix interface, g is the maximum size (diameter) of aggregate, and V_{agg} is the total volume fraction of aggregates. $K_f = \sqrt{g}\,\sigma_f$ corresponds to the highest value of σ at which the two parts of tension-softening curves intersect, provided $\sigma_f \in [\sigma_c, f'_t]$. σ_c follows from the first part of the tension-softening curve by letting $w = w_c = \sqrt{\eta g}$. If a solution is lacking, $K_f = K_c$ is assumed ($K_c = \sqrt{g}\,\sigma_c$), whereby $G_F = G_F^{(1)} + \sqrt{\eta}\,K_c$. The uniaxial tensile strength of concrete f'_t, can be related to the maximum aggregate size of concrete as (Huang & Li, 1989)

$$f'_t = \frac{K_{Ic}}{\sqrt{\pi g/2}} \qquad (3)$$

The effective stress intensity factor of concrete K_{Ic} depends on the operative toughening mechanisms. Thus, the toughening induced by crack deflection, distributed interfacial cracking, and bridging and trapping (Huang & Li, 1989) over and above the matrix toughness, K_{Ic}^m, is given, respectively, by

$$\frac{K_{Ic}}{K_{Ic}^m} = \sqrt{1 + 0.87V} \qquad (4)$$

$$\frac{K_{Ic}}{K_{Ic}^m} = \sqrt{\frac{1}{1-(\pi^2/16)V(1-\nu^2)}} \qquad (5)$$

$$\frac{K_{Ic}}{K_{Ic}^m} = \sqrt{\lambda^2 + \frac{E\left(\frac{\pi}{2}\right)f_{t,a}^2 \cdot g_{av} V\left(1-\sqrt{V}\right)(1-V)\left(1-\nu_m^2\right)}{E_m(1-\nu^2)(K_{Ic}^m)^2}} \qquad (6)$$

where

$$\lambda = \left\{1 - \frac{(1-V)\pi/4}{\ln\{[1+\cos(\pi V/2)]/[\sin(\pi V/2)]\}}\right\}^{-1}$$

$$\frac{E}{E_m} = 1 - \frac{\pi^2}{16}(1-\nu^2)V$$

The relation between E (modulus of elasticity of concrete) and the modulus of elasticity of the matrix, E_m, applies for $\nu=\nu_m$, where ν_m is Poisson's ratio of the matrix. The parameter λ takes the value 1 when the crack trapping mechanism is absent. In the

above expressions, $f'_{t,a}$ is the uniaxial tensile strength of the aggregate and g_{av} is the average aggregate size (diameter). For mortar, the matrix toughness K_{Ic}^{m} would equal that of the cement paste K_{Ic}^{p}, and V would be the volume fraction of the fine aggregate V_f, whereas for concrete, K_{Ic}^{m} would be the fracture toughness of mortar, and V the volume fraction of coarse aggregate V_c.

As the modulus of elasticity of the cement paste is known, E of concrete will be determined using a model proposed by Hobbs (1971). For the determination of K_{Ic}^{p}, linear elastic fracture mechanics based calculation is used. The procedures will be explained below.

5 EXPERIMENTAL DETAILS

The experimental results used in this paper were obtained at the ITU (1996), but here the combined study of experiments and the meso-mechanical approach to the prediction at the fracture and mechanical properties is elaborated.

Table 1. Grading of aggregates and of concrete

Sieve size,	Percentage passing						
mm	16	8	4	2	1	0.5	0.25
Sand	100	100	100	100	100	88	5.6
Limestone fines	100	100	99	59	37	20	6.7
Limestone (4-16)	100	68	15	3	2	1.4	0.7
Grading of concrete	100	91	77	61	53	43	4.6

5.1 *Materials*

Locally available sea sand of the Istanbul area, a Portland cement (PC 42.5), crushed limestone and its fines were used in the mixes. The grading curve of each aggregate is given in Table 1. The particle densities of sand, limestone and limestone fines are 2.60, 2.71, and 2.70, respectively.

In order to determine both the compressive strength and the modulus of elasticity of limestone aggregate, cylindrical specimens were prepared from parent rock; these specimens were 30 mm in diameter and 60 mm high. The modulus of elasticity and compressive strength of limestone were measured at 91.4 GPa and 105.5 MPa, respectively.

5.2 *Mix design*

The grading, water-cement ratio, and maximum aggregate size of concrete were kept constant. The aggregate volume fraction was varied from 0.15 to 0.60 in steps of 0.15. Mix proportions of sand, limestone fines, and limestone were 0.41, 0.32, and 0.27, respectively. Grading curve of concrete is also given in Table 1 together with those of aggregates used in the mixes. Five concrete batches, including cement paste, were made with the same Portland cement, sand and limestone, and its fines. The concretes are designated: M00, M15, M30, M45, and M60, respectively with the number following the letter M indicating the aggregate volume percentage.

All mixes were prepared in a small laboratory mixer with vertical rotation axis by forced mixing. Details of the mixes are shown in Table 2.

All specimens were demoulded after about 24 hours, stored in a water tank, and saturated with lime at about 20°C for 28 days. At least three specimens of each concrete mix were tested under each type of loading condition at 28 days age. For both the modulus of elasticity and standard compressive strength tests, at least three cylinders (100 mm in diameter and 200 mm in height) were used for each mix. For the determination of the critical value of stress intensity factor of hardened cement paste (M00) in Mode I (opening mode) loading, notched disc specimens were used. Table 3 summarizes the test results for the five mixes.

Table 2. Mix proportions and properties of fresh concrete

Mix code	M00	M15	M30	M45	M60
Cement (kg/m^3)	1542	1326	1080	839	597
Sand (kg/m^3)	-	163	323	483	640
Limestone (kg/m^3)	-	131	259	389	514
Crushed limestone (kg/m^3)	-	111	220	323	436
Water (kg/m^3)	487	419	341	265	189
Air (%)	0.5	1.2	1.7	2.0	2.7
Slump (mm)	0	20	23	53	163
Ve Be (sec)	-	12	11	4	2
Water/ Cement	0.316	0.316	0.316	0.316	0.316
Unit weight (kg/m^3)	2030	2150	2223	2305	2376

6 DETERMINATION OF THE CRITICAL VALUE OF SIF K_{IC}^{P} OF HCP (M00)

Disc specimens shown in Figure 4 were made of hardened cement paste (M00) (for mix proportions see Table 2). Two specimen sizes were used to determine K_{Ic}^{P}; diameters 150 mm and 100 mm, and thicknesses 60 mm and 50 mm, respectively. The specimens were cast in a specially designed steel mould; a 2 mm thick steel blade (its length depends on the thickness of the disc) was inserted vertically

Table 3. Mechanical and fracture properties of concretes

Mix Code	Cylinder compressive strength, MPa	Modulus of elasticity, GPa		Effective stress intensity factor, MPa $\sqrt{m}$			Fracture energy $\frac{N}{m}$	Characteristic length, l_{ch} (mm)
		Exp	Model	Fine mortar K_{Ic}^{m1}	Coarse mortar K_{Ic}^{m2}	Concrete K_{Ic}		
M00	91.9	23.2	23.2	0.440	-	-	8.3	-
M15	79.0	27.4	27.7	0.519	0.604	0.704	40.2	55.9
M30	74.7	33.4	33.2	0.554	0.676	0.820	54.4	68.0
M45	76.6	42.1	40.1	0.591	0.755	0.944	72.8	86.6
M60	74.7	46.6	48.8	0.638	0.883	1.132	130	119

through the thickness of the specimen during casting. Several steel blades were used to obtain different a/R ratios. The steel blades were easily removed from the specimens about 4 hours after casting. They were examined to ensure that there was no cracking at the notch tip after the removal of steel blades. The specimens were then cured together with the other specimens. They were also tested at 28 days of age.

In Mode I loading condition, the solution for the normalized load at fracture as a function of the normalized crack length is given by (Yarema & Krestin, 1996),

$$\left\{1+\frac{3}{2}\left(\frac{a}{R}\right)^2+\frac{3}{4}\left(\frac{a}{R}\right)^6+\frac{3}{64}\left(\frac{a}{R}\right)^8\right\}\sqrt{\frac{a}{R}} = K_I\frac{t\sqrt{\pi R}}{P_{cr}} \quad (7)$$

Equation 7 can be re-arranged in the linear form $Y = K_I X$, in which $Y = f\left(\frac{a}{R}\right)$ and $X = t\sqrt{\pi R}/P_{cr}$.

As shown in Figure 5, a linear regression analysis was used to determine the critical value of the SIF, K_{Ic}^P from the slope of the line with a correlation coefficient of 0.91. The values of K_{Ic}^P were close to each other for the two sizes of disc specimens tested. In Figure 6, the critical load P_{cr} has been normalized by using the critical value of SIF, K_{Ic}^P, from disc specimens for different initial notch lengths. It is seen that the experimental results and the analytical LEFM predictions are in excellent agreement. The experimental results obtained for hcp (M00) show that the method of determining K_{Ic}^P described in the present paper can be used as a base for modelling the fracture behaviour of concrete.

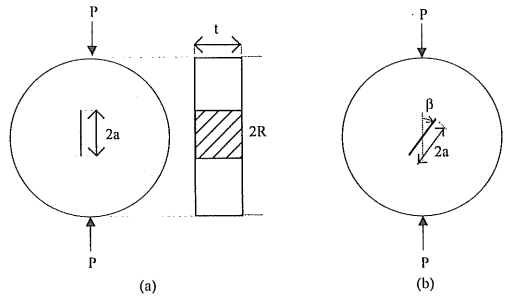

Figure 4. Disc specimens a) Mode I case, b) Mixed mode loading case

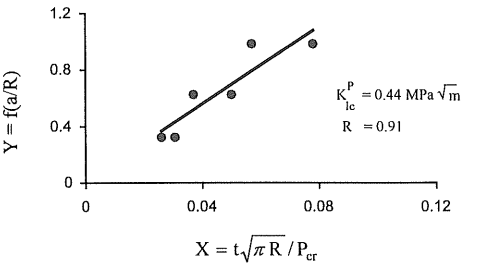

Figure 5. Determination of K_{Ic} for hcp (M00)

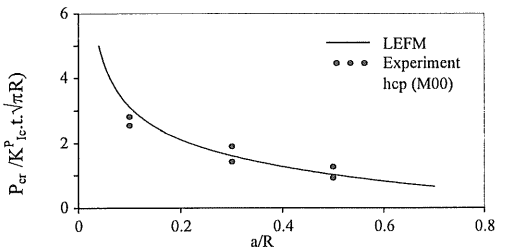

Figure 6. Normalized crack load $P_{cr}/(K^P_{Ic}.t.\sqrt{\pi}R)$ versus normalized crack length (a/R)

7 MESO-MECHANICAL MODELLING OF FRACTURE PARAMETERS

Equations (2)-(6) were used for this modelling, and $G_F^{(2)}$ given in Equations (1) and (2) was neglected, because it had a very low value compared to $G_F^{(1)}$. The following material parameters were chosen for the calculations: $\nu_m = \nu = 0.2$, $g_{av} = 0.25g$, $f'_{t,a} = 10$ MPa for sand and $f'_{t,a} = 9$ MPa for limestone. The maximum particle sizes in fine mortar, coarse mortar

and concrete were 1 mm, 4 mm, and 16 mm, respectively.

7.1 *Effective stress intensity factor* $\left(K_{Ic}^{e}\right)$

In the determination of effective stress intensity factor of each mix, first the effective SIF of fine mortar, K_{Ic}^{m1} (g = 1 mm) was calculated, followed by that of coarse mortar, K_{Ic}^{m2} (g = 4 mm), and finally that of concrete, K_{Ic}^{e}. In each step, water, cement, sand or/and limestone fines, and air content, were in the mortar phase. The effective SIF resulting from any combination of the equations from 4 to 6 were constructed by a simple multiplication of the respective toughening ratios, K_{Ic} / K_{Ic}^{mi}, i.e. i = 1,2, assuming that the mechanisms operate independently. In this analysis, the effective SIF of mortars are enhanced by bridging, crack deflection, and crack trapping, while that of concrete is further enhanced by bridging, deflection, and interfacial cracking. The results obtained are shown in Table 3 and Figure 7. As seen in Figure 7, the effect of the volume fraction of sand in the fine mortar (Mortar m1) is not very significant, and linear elastic fracture mechanics can be used for the determination of K_{Ic} for this type of mortar. However, in coarse mortar (g = 4 mm) there is a definite increase in the SIF K_{Ic}^{m2} with the aggregate volume fraction. The increase is particularly noticeable in concrete (g = 16 mm) for which the SIF K_{Ic} is significantly higher than that of coarse mortar (g = 4 mm). Figure 7 proves that linear elastic fracture mechanics cannot be applied for the determination of SIFs of coarse mortar and, especially of concrete. It can be also concluded that the meso-mechanical relations used in this study are very useful tools for gaining a better understanding of material behaviour.

7.2 *Fracture Energy (G_F)*

The fracture energy (G_F) given by Equation 2 is calculated assuming that $G_F^{(1)} = G_F$. In the calculation of G_F, the effective SIF of concrete and the total volume fraction of aggregate in concrete

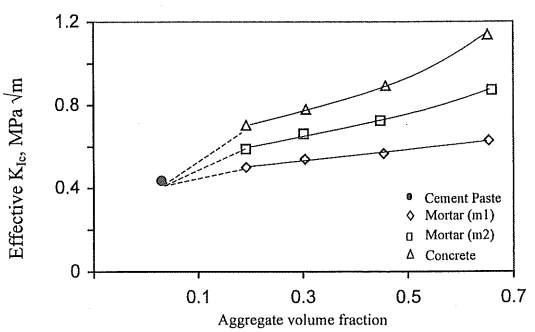

Figure 7. Effective SIF versus aggregate volume fraction

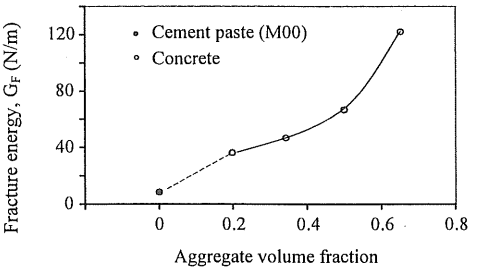

Figure 8. Fracture Energy (G_F) versus aggregate volume fraction

were used. As seen from Table 3 and Figure 8, there is a substantial increase in the fracture energy (G_F) with an increase in the aggregate volume fraction. The fracture energy of hardened cement paste (M00), however, is calculated based on the LEFM. The variation of G_F in the very wide range of aggregate content is significant. The results obtained also show that the enhancement of fracture energy by adding aggregates from 0.00 to 0.60 is substantial as expected in the brittle matrix composites such as concrete.

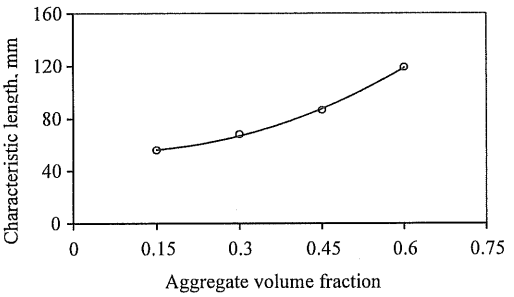

Figure 9. Characteristic length versus aggregate volume fraction

7.3 *Characteristic Length (l_{ch})*

The characteristic length of concrete, l_{ch}, is given by the following expression

$$l_{ch} = \frac{G_F E}{f_t'^2}$$

where G_F is the fracture energy, E is the modulus of elasticity, and f_t' is the uniaxial tensile strength of concrete. As seen from Table 3 and Figure 9, as the aggregate volume fraction increases, the characteristic length, which is a measure of ductility of the mix, increases significantly.

The meso-mechanical modelling approach used in this study gives a clear picture of how a brittle matrix (i.e. hcp) transforms progressively into a ductile composite with the addition of fine and coarse aggregates, the ductility (as measured by l_{ch})

increasing as the volume fraction of aggregates is increased.

8 CONCLUSIONS

Based on the meso-mechanical relations and experimental data, the following conclusions can be drawn:

1°) The effect of the aggregate volume fraction on the effective stress intensity factor of fine mortar is not significant; there is however a noticeable increase in that of coarse mortar. On the other hand, the effective stress intensity factor of concrete is strongly affected by the aggregate volume fraction.

2°) The toughening mechanisms are very important in the fracture of concrete; they should be taken into account when the fracture parameters of concrete are determined.

3°) The meso-mechanical relations used in this study are very useful tools for gaining a better understanding of how a brittle hardened cement paste progressively transforms into a quasi-brittle concrete.

4°) The compressive strength decreases with an increase in the aggregate volume fraction V, up to $V = 0.5$, whereafter it remains practically constant.

5°) As the aggregate volume fraction increases, the modulus of elasticity, the splitting tensile strength, the effective stress intensity factor, the fracture energy, and the characteristic length all increase.

9 ACKNOWLEDGEMENT

The work presented here was completed at Cardiff University (CU), Wales. The first author wishes to acknowledge the financial support of CU during his visit.

10 REFERENCES

Aitcin P.C. & Mehta P.K. 1990. Effect of coarse aggregate characteristics on Mechanical properties of high strength concrete. *ACI Materials Journal*, 88(2): 103-107.

Baalbaki W., Benmokrane B., Chaallal O. & Aitcin P.C. 1991. Influence of coarse aggregate on elastic properties of high performance concrete. *ACI Materials Journal*, 87(5): 499-503.

Hillerborg A., Modeer M. & Petersson P.E. 1976. Analysis of crack formation and crack growth in concrete by means of fracture mechanics and finite elements. *Cement and Concrete Research*, 5(6): 773-784.

Hobbs D.W. 1971. The dependence of the bulk modulus, creep, shrinkage and thermal expansion of concrete upon aggregate volume concentration. *Materials and Structures*, 4(20): 107-114.

Huang J. & Li V.L. 1989. A meso-mechanical model of the tensile behaviour of concrete Part II: Modelling of post-peak tension softening behaviour. *Composites*, 20(4): 370-378.

Karihaloo B.L. 1995. Fracture mechanics and structural concrete. Addison Wesley Longman , England.

Karihaloo B.L., Fu D. & Huang X. 1991. Modelling of tension softening in quasi-brittle materials by an array of circular holes with edge cracks. *Mechanics of Materials*, 11: 123-134.

Lange-Kornbak D. & Karihaloo B.L. 1996. Design of concrete mixes for minimum brittleness. *Advanced Cement Based Materials*, 3: 124-132.

Lange-Kornbak D. & Karihaloo B.L. 1999. Role of microstructural parameters in the properties of plain concrete. *Concrete Science and Engineering*, RILEM, 1: 238-252.

Larbi I.A. 1993. Microstructure of the interfacial zone around aggregate particles in concrete. *Heron*, Delft, 38(1).

Neville A.M. 1997. Aggregate bond and modulus of elasticity of concrete. *ACI Materials Journal*, 94(1): 71-74.

Sarisu F. 1996. Effect of aggregate concentration on the mechanical properties of concrete. MS Thesis, Istanbul Technical University.

Sarkar S.L. 1994. The importance of microstructure in evaluating concrete. In V.M. Malhotra (ed.), *Advances in concrete technology*, Second edition, CANMET, Ottawa, 125-160.

Sengül Ö., Tasdemir C., Tasdemir M.A., Hacikamiloglu M., Özbek E. & Altay B. 2000. Effect of aggregate type on mechanical properties of normal and high strength concretes. In A. Yeginobali (ed.), *Cement and Concrete Technology in 2000s,* TCMA, Second International Symposium, 6-10 Sept. 2000, Istanbul, 2: 40-49.

Shah S.P., Ouyang C. & Swartz S.E. 1995. Fracture mechanics of concrete: Applications of fracture mechanics to concrete, rock, and other brittle materials. John Wiley and Sons, Inc., New York.

Skalny J.P. (ed.), 1989. Materials Science of Concrete I. The American Ceramic Society, Westerville, OH.

Tasdemir C., Tasdemir M.A., Barr B.I.G. & Lydon F.D. 1996. Effects of silica fume and aggregate size on the brittleness of concrete. *Cement and Concrete Research*, 26(1): 63-58.

Tasdemir C., Tasdemir M.A., Grimm R. & König G. 1995. Microstructural effects on the brittleness of high strength concretes. In F.H. Wittmann (ed.), *Fracture Mechanic of Concrete Structures*, Proc. FRAMCOS-2, Aedificatio Publishers, Freiburg, 125-134.

Tasdemir C., Tasdemir M.A., Mills N., Barr B.I.G. & Lydon F.D. 1999. Combined effects of silica fume, aggregate type and size on post-peak response of concrete in bending. *ACI Materials Journal*, 96(1): 74-83.

Van Mier J.G.M. 1991. Mode I fracture of concrete: Discontinuous crack growth and crack interface grain bridging. *Cement and Concrete Research*, 21: 1-15.

Wittmann F.H. 1983. Structure of concrete with respect to crack formation. In F.H. Wittmann (ed.), *Fracture mechanics of concrete*, Elsevier Applied Science, Amsterdam, 43-74.

Yarema S.Ya. & Krestin G.S. 1966. Determination of the modulus of cohesion of brittle materials by compressive tests on disc specimens containing cracks. *Fiziko-Khimicheskaya Mekhanika Materialov*, 2(1): 10-14.